Synthesis, characterization and reactivity of carbohydrate platinum(IV) complexes with thioglycoside ligands†

Cornelia Vetter,[a] Papapida Pornsuriyasak,[b] Jürgen Schmidt,[c] Nigam P. Rath,[b] Tobias Rüffer,[d] Alexei V. Demchenko*[b] and Dirk Steinborn*[a]

Received 23rd December 2009, Accepted 16th April 2010
First published as an Advance Article on the web 1st June 2010
DOI: 10.1039/b927058b

Reactions of *fac*-[$PtMe_3$(4,4′-R_2bpy)(Me_2CO)][BF_4] (R = H, **1a**; ^{t}Bu, **1b**) and *fac*-[$PtMe_3$-(OAc-κ^2*O*,*O*′)(Me_2CO)] (**2**), respectively, with thioglycosides containing thioethyl (ch-SEt) and thioimidate (ch-STaz, Taz = thiazoline-2-yl) anomeric groups led to the formation of the carbohydrate platinum(IV) complexes *fac*-[$PtMe_3$(4,4′-R_2bpy)(ch*)][BF_4] (ch* = ch-SEt, **8–14**; ch-STaz, **15–23**) and *fac*-[$PtMe_3$(OAc-κ^2*O*,*O*′)(ch*)] (ch* = ch-SEt, **24–28**; ch-STaz = **29–35**), respectively. NMR (^{1}H, ^{13}C, ^{195}Pt) spectroscopic investigations and a single-crystal X-ray diffraction analysis of **19** (ch-STaz = 2-thiazolinyl 2,3,4,6-tetra-*O*-benzoyl-1-thio-β-D-galactopyranose) revealed the *S* coordination of the ch-SEt glycosides and the *N* coordination of the ch-STaz glycosides. Furthermore, X-ray structure analyses of the two decomposition products *fac*-[$PtMe_3$(bpy)(STazH-κ*S*)][BF_4] (**21a**) and 1,6-anhydro-2,3,4-tri-*O*-benzoyl-β-D-glucopyranose (**23a**), where a cleavage of the anomeric C–S bond had occurred in both cases, gave rise to the assumption that this decomposition was mediated due to coordination of the thioglycosides to the high electrophilic platinum(IV) atom, in non-strictly dried solutions. Reactions of *fac*-[$PtMe_3$(Me_2CO)$_3$][BF_4] (**3**) with ch-SEt as well as with ch-SPT and ch-Sbpy thioglycosides (PT = 4-(pyridine-2-yl)-thiazole-2-yl; bpy = 2,2′-bipyridine-6-yl), having *N*,*S* and *N*,*N* heteroaryl anomeric groups, respectively, led to the formation of platinum(IV) complexes of the type *fac*-[$PtMe_3$(ch*)][BF_4] (ch* = ch-SEt, **36–40**, ch-SPT **42–44**, ch-Sbpy **45**, **46**). The thioglycosides were found to be coordinated in a tridentate κ*S*,κ^2*O*,*O*′, κ*S*,κ*N*,κ*O* and κ*S*,κ^2*N*,*N*′ coordination mode, respectively. Analogous reactions with ch-STaz ligands succeeded for 2-thiazolinyl 2,3,4-tri-*O*-benzyl-6-*O*-(2,2′-bipyridine-6-yl)-1-thio-β-D-glucopyranoside (**5h**) resulting in *fac*-[$PtMe_3$(ch-STaz)][BF_4] (**41**, ch-STaz = **5h**), having a κ^3*N*,*N*′,*N*″coordinated thioglycoside ligand.

1. Introduction

Carbohydrates are one of the most important classes of biomolecules. Attached to lipids, proteins and nucleobases they exert versatile functions in living organisms, ranging from immune defence and cell growth to inflammation and malignant transformations.[1,2] Carbohydrate-based pharmaceuticals have been proven to be promising therapeutics for neurodegenerative diseases, because they can easily pass the blood brain barrier.[3] Thiofunctionalized carbohydrates were proved to possess significant bioactivity. It was found that 5-thio-β-D-glucopyranose, where the ring oxygen is replaced by sulfur, can cause temporary diabetes and sterility in rats.[4] Moreover, this carbohydrate class, having a ring sulfur atom, exhibit cancerostatic properties[5] and act as enzyme inhibitors.[6] Up to now, it has also been shown that thioglycosides and carbohydrates with mercapto groups instead of hydroxyl groups are enzyme inhibitors and thereby possess antiproliferative and anti-inflammatory properties.[7] Metal-coordination of carbohydrates also plays a significant role in biosyntheses, including metal transportation and storage or the regulation of metalloenzymes.[8,9] Furthermore, metal–carbohydrate complexes have been investigated as potent radiopharmaca[10] and cancerostatica, where platinum compounds are of considerable interest.[11] From a coordination chemistry perspective the syntheses of carbohydrate platinum(IV) complexes, particularly with non-functionalized carbohydrate ligands, represent a notable challenge, due to their weak donor ability and their propensity to act as reducing agents.[12] On the other hand, platinum(IV) complexes are kinetically inert due to the low-spin d^6 electron configuration, so substitution reactions are not favored. However, numerous platinum(IV) complexes with neutral carbohydrate ligands have been synthesized using trimethylplatinum(IV) precursor complexes such as *fac*-[$PtMe_3$(Me_2CO)$_3$][BF_4]. Complexes of this type have proven especially useful in this respect because the high donor capability of the methyl ligands stabilizes

[a]*Institut für Chemie – Anorganische Chemie, Martin-Luther-Universität Halle-Wittenberg, D-06120, Halle, Kurt-Mothes-Straße 2, Germany. E-mail: dirk.steinborn@chemie.uni-halle.de; Fax: +49345 5527028; Tel: +49345 5525620*
[b]*Department of Chemistry and Biochemistry, University of Missouri-St. Louis, 63121, Missouri, One University Boulevard, USA. E-mail: demchenkoa@umsl.edu; Tel: +1314 5167995*
[c]*Leibniz-Institut für Pflanzenbiochemie, D-06120, Halle, Weinberg 3, Germany*
[d]*Institut für Chemie – Technische Universität Chemnitz, D-09111, Chemnitz, Straße der Nationen 62, Germany*

† Electronic supplementary information (ESI) available: Experimental data for *fac*-[$PtMe_3$I(4,4′-^{t}Bu_2bpy)]. Spectroscopic data for complexes **1–46**. Energies and Cartesian coordinates calculated for equilibrium structures **2** and **2′**. CCDC reference numbers 758897–758899. For ESI and crystallographic data in CIF or other electronic format see DOI: 10.1039/b927058b

the platinum(IV) oxidation state. Furthermore, the leaving ligands (acetone) are only weakly coordinated and their substitution is additionally facilitated by the high *trans* effect of the methyl ligands.[13] Herein we present the synthesis, characterization and reactivity of various types of trimethylplatinum(IV) complexes with thioglycoside ligands.

2. Results and discussion

2.1. Starting complexes and ligands

For the synthesis of trimethylplatinum(IV) complexes with thioglycoside ligands, starting complexes having up to three substitution-labile ligands were used. Complexes with one substitution-labile acetone ligand, *fac*-[$PtMe_3(Me_2CO)(bpy)$][BF_4] (**1a**) and *fac*-[$PtMe_3(Me_2CO)(4,4'$-^{t}$Bu_2bpy)$][BF_4] (**1b**; Scheme 1), were prepared by the reaction of *fac*-[$PtMe_3I(bpy)$] and *fac*-[$PtMe_3I(4,4'$-^{t}$Bu_2bpy)$], respectively, with Ag[BF_4].[14] The reaction of the tetranuclear heterocubane complex *fac*-[$(PtMe_3I)_4$] with AgOAc resulted in the formation of *fac*-[$PtMe_3(OAc)(Me_2CO)_n$] (**2**). The acetato ligand can be bidentately or monodentately coordinated (OAc-κ^2O,O', $n = 1$; OAc-κO, $n = 2$). DFT calculations showed that the free energy at 298 K of the reaction

$$fac\text{-}[PtMe_3(OAc\text{-}\kappa O)(Me_2CO)_2] \rightleftharpoons fac\text{-}[PtMe_3(OAc\text{-}\kappa^2O,O')(Me_2CO)] + Me_2CO$$

amounts to be –44 kJ mol^{-1} in the gas phase and –61 kJ mol^{-1} in acetone. This gives proof that the acetato ligand is bidentately bound. Nevertheless, both complexes have at their disposal up to three substitution-labile coordination sites, namely one when the acetone ligand is cleaved off and the acetato ligand is still coordinated in a chelating binding fashion, two when the acetone ligand is cleaved off and the acetato ligand remains to be κ^1O coordinated or three in the case of complete cleavage of the acetato ligand.

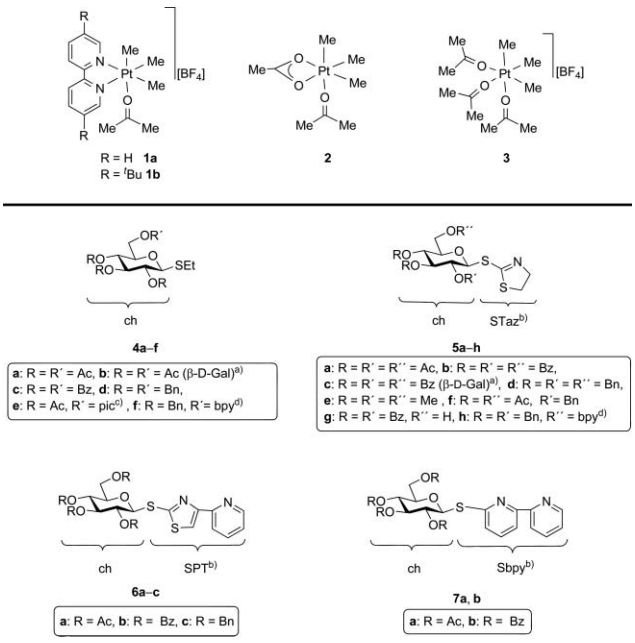

Scheme 1 Platinum(IV) precursor complexes and β-D-thioglycosides used as ligands. [a] β-D-Galactose: OR at C4 in axial position. [b] Abbreviations: ch-STaz: Taz = thiazoline-2-yl; ch-SPT: PT = 4-(pyridine-2-yl)-thiazole-2yl; ch-Sbpy: bpy = 2,2′-bipyridine-6-yl. [c] pic: 2-picoline-2-yl. [d] bpy_{-H}: 2,2′-bipyridine-6-yl.

The analogous reaction of *fac*-[$(PtMe_3I)_4$] with Ag[BF_4] led to *fac*-[$PtMe_3(Me_2CO)_3$][BF_4] (**3**; Scheme 1), which possesses three substitution-labile acetone ligands.[13] It should be noted that all complexes described here were synthesized *in situ* and used directly for reactions with thioglycosides which are summarized in Scheme 1. Four different classes of thioglycosides have been investigated, namely those with SEt anomeric groups ch-SEt (**4a–f**) and those having *N*,*S* or *N*,*N* heterocyclic anomeric groups: ch-STaz (**5a–h**; Taz = thiazoline-2-yl), ch-SPT (**6a–c**; PT = 4-(pyridine-2-yl)-thiazole-2-yl) and ch-Sbpy (**7a**,**b**; bpy = 2,2′-bipyridine-6-yl).

2.2. Cationic platinum(IV) complexes with monodentately coordinated thioglycoside ligands

Syntheses and X-ray diffraction analysis. Complexes **1a** and **1b** reacted in acetone with stoichiometric amounts of thioglycosides of type **4** and **5** (Scheme 1) yielding ionic complexes of the type *fac*-[$PtMe_3(4,4'$-R_2bpy)(ch-SEt-κS)][BF_4] (R = H: **8–11**; R = ^{t}Bu: **13**, **14**) and *fac*-[$PtMe_3(4,4'$-R_2bpy)(ch-STaz-κN)][BF_4] (R = H: **17–23**; R = ^{t}Bu: **15**, **16**), respectively (Scheme 2, Table 1). The complexes were isolated as moderately air-stable yellow and white powders, respectively, in yields of 45–94%. All complexes were characterized by ^{1}H, ^{13}C and ^{195}Pt NMR spectroscopy as well as by IR spectroscopy, high resolution ESI mass spectrometry and in the case of **19** also by X-ray diffraction analysis.

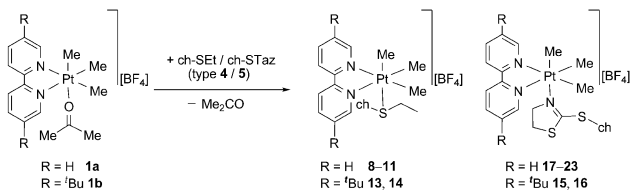

Scheme 2 Syntheses of carbohydrate platinum(IV) complexes *fac*-[$PtMe_3(4,4'$-R_2bpy)(ch*)][BF_4] (ch* = ch-SEt, R = H **8–11**, R = ^{t}Bu **13**, **14**; ch-STaz, R = H **17–23**, R = ^{t}Bu **15**, **16**).

Small colorless needles of *fac*-[$PtMe_3$(bpy)(ch-STaz)][BF_4] (**19**; ch-STaz = **5c**) were formed in an acetone solution layered with tetrahydrofuran and diethyl ether. Complex **19** crystallized in the chiral space group $P4_12_12$. The asymmetric unit consists of two symmetry independent *fac*-[$PtMe_3$(bpy)(ch-STaz)]$^+$ (ch-STaz = **5c**) cations, and two [BF_4]$^-$ anions, wherein one exhibits a disorder. In Fig. 1, only one of the cations is illustrated, whereas the other one exhibits a similar structure. Selected bond lengths and angles are given in the figure caption. In complex **19** the platinum atom [PtC_3N_3] is octahedrally coordinated by three methyl ligands in *facial* arrangement, a bipyridine ligand and the thiazoline-2-yl ring, which is coordinated *via* the nitrogen atom. The angle between the thiazoline-2-yl ring and the equatorial [PtC_2N_2] plane is nearly perpendicular (86.5/89.8°‡). The Pt–N bond length (2.16(1)/2.17(2) Å) belongs to the longest bonds known for Pt(IV)–N(CH_2)=C complexes (median: 2.139 Å, lower/upper quartile:

‡ The values of the two symmetry independent molecules are given separated by a slash.

Table 1 ^{1}H and ^{13}C NMR spectroscopic data (δ in ppm, J in Hz) of the methyl ligands and ^{195}Pt chemical shifts of the complexes *fac*-[$PtMe_3$(bpy)(ch*)][BF_4] (**8–12**; **17–23**) and *fac*-[$PtMe_3$(4,4′-^{t}Bu_2bpy)(ch*)][BF_4] (**13–16**)

		δ_H		δ_C		$^1J_{Pt,C}$		$^2J_{Pt,H}$		
Complex	ch*	*trans* ch*	*trans* N_{bpy}	*trans* ch*	*trans* N_{bpy}	*trans* ch*	*trans* N_{bpy}	*trans* ch*	*trans* N_{bpy}	δ_{Pt}
	ch-SEt									
8	**4a**	0.66	1.09	5.8	−5.0/−5.1	662.0	657.0./658.3	72.0	67.8	−2772
9	**4b**	0.65	1.09/1.11	5.1	−5.1/−5.4	652.0	662.0/654.5	71.6	69.3/67.8	−2529
10	**4c**	0.71	1.16	5.4	−4.5/−4.7	660.0	657.3/662.8	72.3	67.5	−2447
11	**4d**	0.64	1.14/1.16	5.1	−5.1/−5.2	649.5	663.2/662.0	71.0	66.9/66.9	−2446
12	**4e**	0.68	1.18/1.19	5.2	−4.6/−4.7	648.4	662.2/661.5	71.1	67.4/67.4	−2469
13	**4a**	0.66	1.03/1.10	5.8	−5.2/−5.3	647.1	659.4/664.6	72.6	66.4/67.1	−2769
14	**4c**	0.59	1.04	5.8	−5.0/−5.2	658.3	655.8/662.0	72.2	68.2	−2435
	ch-STaz									
15	**5c**	0.53	1.13	−5.4	−3.3	678.2	675.7	71.4	68.1	−2716
16	**5g**	0.32	0.83/1.02	−6.1	−3.2/−4.7	676.6	667.0/684.4	72.5	67.6/66.9	−2452
17	**5a**	0.45	1.13/1.17	−5.5	−3.2/−4.2	673.1	677.0/677.8	72.2	68.5/67.2	−2730
18	**5b**	0.38	0.93/1.08	−5.7	−3.6	672.4	676.2	72.2	67.2/67.2	−2683
19	**5c**	0.39	0.93/1.08	−5.7	−3.6/−4.2	674.4	678.2/676.9	72.2	67.2/68.1	−2710
20	**5d**	0.45	1.21/1.23	−5.7	−3.7/−4.0	674.3	679.4/679.3	72.2	67.2/68.1	−2695
21	**5e**	0.42	1.18/1.19	−5.5	−4.0/−4.1	673.8	680.6/680.7	72.2	67.2/68.1	−2704
22	**5f**	0.42	1.19	−5.6	−3.7/−4.1	677.5	679.4/679.8	72.2	68.1	−2444
23	**5g**	0.37	0.93/1.06	−5.7	−3.6/−4.2	678.5	679.4/675.6	72.2	67.2/67.2	−2445

2.049/2.163 Å, n = 36; n – number of observations[15]), likely due to the high *trans* influence of the methyl ligands.[13,16] The STaz ring exhibits a distorted half-chair conformation, while the pyranose ring assumes a distorted chair conformation.[17] A complex hydrogen bond network of moderate to weak inter- and intramolecular hydrogen bonds of the types C–H···O, C–H···F and C–H···S, respectively, is found in crystals of **19**.

NMR spectroscopic characterization of the complexes 8–23. The ^{1}H and ^{13}C NMR spectra of complexes **8–23** showed unambiguously the coordination of the thioglycosides. Due to the coordination of the chiral carbohydrates to the platinum atom the complexes exhibited C_1 symmetry. Thus, a double signal set for the two halves of the bipyridine ligand, as along with the methyl ligands in *trans* position to the bipyridine ligand could be observed (Table 1). However, the chemical shifts of the methyl ligands were still very similar, leading to coincidence of signals for some compounds (Table 1). Coordination of the carbohydrates in complexes **8–23** led to a partial broadening of the signals of the carbohydrate protons and carbon atoms at room temperature, which has been proven to be characteristic for carbohydrate coordination also in other carbohydrate platinum(IV) complexes.[13] A general shift of the resonances of the carbohydrate protons to higher field was observed for the complexes **8–23**. Furthermore, the shift differences of the signals for the two protons belonging to the CH_2 groups of the SEt and STaz moieties were significantly increased due to the coordination to the platinum atom. On the other hand, only marginal coordination-induced shifts (CIS ≤ 1.6 ppm) for the resonances of the pyranose ring carbon atoms could be found.

In the case of complexes **8–11**, **13** and **14** the *S* coordination of the SEt group gave rise to upfield shifts of the CH_2 proton signals of the SEt group up to 0.32 ppm and of the H1 protons up to 0.11 ppm. Interestingly, the coordination-induced shifts both of the carbon atom resonances of the Et group and of the anomeric C atom resonances were small (≤ 1.0 ppm) with the exception of complex **11**, where the carbon atom of the methylene group was shifted upfield by 1.9 ppm. For complex **12**, wherein thioglycoside **4e**, having an additional *N*-donor site (picoline-2-yl), was used, the coordination mode could not be unambiguously assigned. On the one hand, the picoline-2-yl resonances in the ^{1}H and ^{13}C NMR spectra are shifted downfield up to 0.2 and 2.4 ppm, respectively, which indicated an *N* coordination. Conversely, the broadening and increase of the shift differences for the signals of the CH_2 group of the SEt moiety in the ^{1}H NMR spectrum, as well as the $^1J_{Pt,C}$ coupling constant of the methyl ligand in *trans* position to the thioglycoside ligand of 648.4 Hz, indicated an *S* coordination.

In the case of complexes **15–23** the κ*N* coordination of the STaz moiety has been proven unambiguously by the X-ray structure analysis of complex **19**. Comparison of ^{1}H and ^{13}C NMR data of complex **19** with those of the other complexes clearly demonstrated that the complexes **15–18** and **20–23** also possess bound κ*N* coordinated ligands. Without the structural information on complex **19** it would be impossible to derive the coordination mode solely based on the NMR data. The signals for the NCH_2 and H1 protons showed the greatest CIS's (up to 0.98 ppm and 0.57 ppm, respectively). On the other hand, the carbon atom resonances of the SCH_2 groups were strongly shifted upfield (up to 3.4 ppm), whereas the carbon atom resonances of the NCH_2 groups were only marginally shifted (up to 0.4 ppm).

The ^{1}H and ^{13}C NMR signals of the methyl ligands *trans* to the thioglycoside ligands of type **4** were found in the range of 0.59–0.71 and 5.1–5.8 ppm, respectively. The requisite signals in complexes **15–23** with carbohydrate ligands of type **5** were found upfield shifted, with the shifts ranging from 0.32–0.53 ppm and −5.4 to −6.1 ppm, respectively. It had been shown, that the $^1J_{Pt,C}$ coupling constants in complexes of this type can be regarded to be a measure for the *trans* influence.[16] The comparison of the $^1J_{Pt,C}$ couplings constants of the methyl ligands *trans* to the carbohydrate ligands in complexes **8–14** (647.1–662.0 Hz) with those in complexes **15–23** (672.4–678.5 Hz) indicated a higher *trans* influence of the thioglycosides with the SEt group than that of the respective

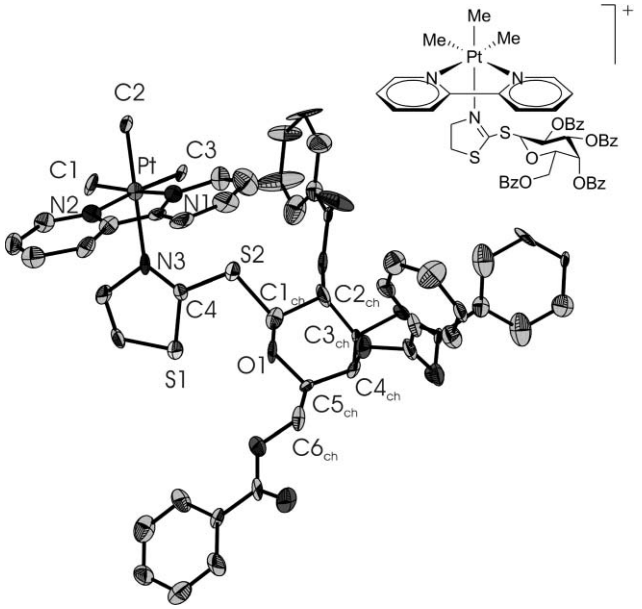

Fig. 1 Molecular structure of one of the two crystallographically independent cations of *fac*-[$PtMe_3$(bpy)(ch-STaz-κ*N*)][BF_4] (**19**, ch-STaz = **5c**). Hydrogen atoms are omitted for clarity. The ellipsoids are drawn at the 30% probability level. Selected bond lengths (in Å) and angles (in °)[a]: Pt–C1 2.14(2)/2.03(1), Pt–C2 1.98(1)/2.07(2), Pt–C3 2.02(2)/2.05(2), Pt–N3 2.16(1)/2.17(2), N3–C4 1.30(2)/1.33(2), C4–S2 1.73(2)/1.67(2), $C1_{ch}$–S2 1.85(2)/1.82(2), $C1_{ch}$–$C2_{ch}$ 1.55(2)/1.64(2), $C2_{ch}$–$C3_{ch}$ 1.51(2)/1.56(2), $C3_{ch}$–$C4_{ch}$ 1.44(2)/1.54(2), $C4_{ch}$–$C5_{ch}$ 1.43(2)/1.70(2), $C5_{ch}$–O1 1.41(2)/1.51(2), $C1_{ch}$–O1 1.42(2)/1.42(2), C1–Pt1–C2 88.8(6)/84.5(8), C2–Pt1–N3 179.5(6)/174.0(8), C3–Pt1–N2 175.3(6)/177.2(6), C4–S2–$C1_{ch}$ 104.6(8)/101.8(9), $C1_{ch}$–O1–$C5_{ch}$ 111(1)/117(1), O1–$C1_{ch}$–$C2_{ch}$ 111(2)/111(2), $C1_{ch}$–$C2_{ch}$–$C3_{ch}$ 104(1)/107(1), $C2_{ch}$–$C3_{ch}$–$C4_{ch}$ 113(2)/117(2), $C4_{ch}$–$C5_{ch}$–O1 116(1)/104(1).[a] The values of the two symmetry independent molecules are given separated by a slash.

STaz functionalized glycosides. Comparison with data given in the literature revealed that SEt carbohydrates in **8–14** possess a similar *trans* influence like in analogous platinum(IV) complexes having thionucleobase ligands *fac*-[$PtMe_3$(bpy)L][BF_4] (L = SCy, 1-MeSCy, s^4Ura, s^2s^4Ura; $^1J_{Pt,C}$: 642.1–651.5 Hz).[18] The respective values in the complexes **15–23** were also found in accordance with those observed for trimethyl platinum(IV) complexes having *N*-bound ligands like 2-(methylthio)-2-thiazoline and pyrrazole in *trans* position ($^1J_{Pt,C}$: 675.4, 682.3 Hz).[19] ^{195}Pt chemical shifts for complexes **8–23** (Table 1) were found to be in the same range as for other trimethyl(bipyridine)platinum(IV) complexes.[16,18] Between complexes **8–14** (–2435 to –2772 ppm) and **15–23** (–2444 to –2730 ppm) no distinct shift differences were found. Thus, differences in the donor strength of the carbohydrate ligands seems to be too small to be clearly reflected in the δ_{Pt} values.

On the decomposition of the carbohydrate platinum(IV) complexes. Under strictly dehydrated conditions solutions of the complexes **8–23** were stable over weeks. Within two to three months only a slow decomposition with formation of platinum black took place, as indicated by NMR spectroscopy. In contrast, solutions in acetone, which were not strictly dehydrated, were found to be less stable. Thus, a solution of *fac*-[$PtMe_3$(bpy)(ch-STaz-κ*N*)][BF_4] (**21**, ch-STaz = **5e**) was found to decompose with the formation of well-shaped crystals, which were suitable for X-ray diffraction analysis. The compound **21a** crystallized in the space group $P2_1/c$. The asymmetric unit consists of a *fac*-[$PtMe_3$(bpy)(STazH-κ*S*)]$^+$ cation and a disordered tetrafluoroborate anion. The molecular structure of the cation of **21a** is shown in Fig. 2. Selected bond lengths and angles are given in the figure caption. The primary donor set [PtC_3N_2S] of the octahedrally coordinated platinum atom is built up by three methyl ligands in *facial* arrangement, the bipyridine ligand and the thiazolidine-2-thione (STazH) ligand, which is coordinated *via* the exocyclic sulfur atom to the platinum atom. The five membered heterocycle possesses a distorted half chair conformation along the C12–C13 bond, based on the torsion angle concept.[17] Compared to the C=S bond in the free ligand (1.671–1.680 Å[20]) no significant coordination-induced lengthening can be observed. Thus, the C11–S bond (1.683(4) Å) in complex **21a** exhibits double bond character. In accordance with the high *trans* influence of the methyl ligands, the Pt1–S1 bond length (2.4818(9) Å) belongs to the longest ones known, as compared with thioketone platinum(IV) complexes (median: 2.372 Å, lower/upper quartile: 2.312/2.474 Å; $n = 9$,[15]). The interplanar angle between the STazH ligand and the equatorial [PtC_2N_2] plane is 75.7°. As shown in Fig. 3, cation–anion interactions in crystals of **21a** are related to hydrogen bond interactions of the type N3–H···F2 (N3···F2 2.854(4) Å). Furthermore, molecules of **21a** are packed like a "staircase" in infinite columns (Fig. 3). The distances between the bpy ligands (3.79/3.81 Å) together with the displacement§ angle of 26.2° and 25.1°, respectively, indicated a weak stabilization through π–π and/or σ–π (C–H···π) interactions.[21]

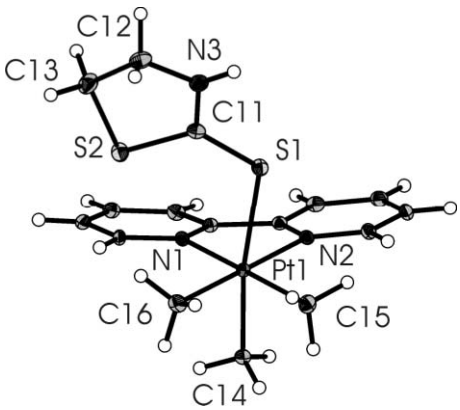

Fig. 2 Molecular structure of the cation of *fac*-[$PtMe_3$(bpy)-(STazH-κ*S*)][BF_4] (**21a**). The ellipsoids are drawn at the 30% probability level. Selected bond lengths (in Å) and angles (in °): Pt–C15 2.050(3), Pt–C16 2.048(3), Pt–C14 2.046(3), Pt–N1 2.155(2), Pt–N2 2.163(3), Pt–S1 2.4818(9), C11–S1 1.683(4), N1–Pt–N2 76.4(1), C15–Pt–C16 85.5(2), C14–Pt–N2 90.0(1), S1–Pt–C14 172.12(9), C15–Pt–N1 173.9(1), C11–S1–Pt 117.0(1).

Most likely, complex **21a** is a product of the hydrolysis of **21**, which was induced by traces of water in the reaction mixture, followed by an isomerization (Scheme 3(a)). The cleavage of the glycosidic bond in **21** gave proof for the platinum mediated activation of the glycosidic bond due to coordination to the

§ The displacement, measured by the angle between the ring normal and the centroid–centroid vector, is a measure for the ring–ring overlap.

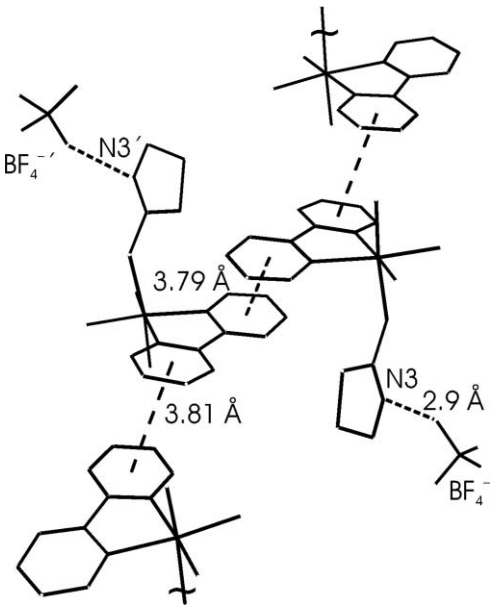

Fig. 3 Solid state structure of *fac*-[$PtMe_3$(bpy)(STazH-κ*S*)][BF_4] (**21a**) showing the packing of the cations by π–π stacking (---) and the hydrogen bonds (···) between cations and anions. Hydrogen atoms are omitted for clarity. Only one of the two disordered positions of the fluorine atoms are shown.

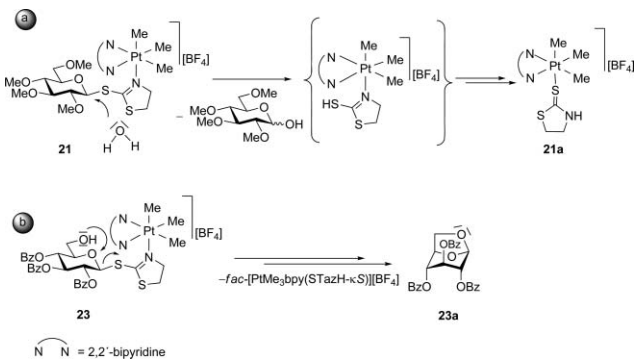

Scheme 3 Possible mechanisms for the decomposition of **21** to **21a** (a) and **23** to **23a** (b).

electrophilic cationic Pt(IV) center. Another indication for this is the product of hydrolysis, obtained in the reaction of complex **1a** with 2-thiazolinyl 2,3,4-tri-*O*-benzoyl-1-thio-β-D-glucopyranose (**5g**). Crystals of a decomposition product (1,6-anhydro-2,3,4-tri-*O*-benzoyl-β-D-glucopyranose, **23a**) were obtained from the acetone mother liquor. X-Ray diffraction analysis revealed that **23a** crystallizes in the space group *P*1. The unit cell consists of two symmetry independent, but structurally very similar, molecules. The molecular structure of one molecule is depicted in Fig. 4. Selected bond lengths and angles are given in the figure caption. The pyranose ring possesses a distorted chair conformation on O1 and C3, while the five membered ring exhibits an envelope conformation on O1.[17] The anhydro moiety was most likely formed due to an intramolecular nucleophilic attack of the oxygen atom O6 belonging to the unprotected hydroxyl group at C6, whereas the glycosidic bond was activated by platinum coordination, as discussed above (Scheme 3(b)).

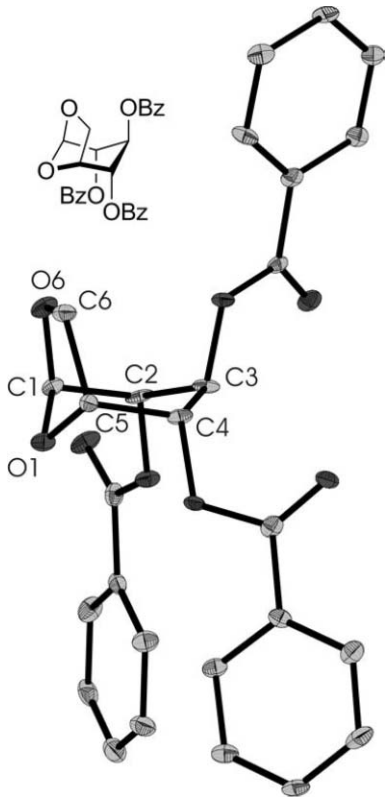

Fig. 4 Molecular structure of one of the two symmetry independent molecules of 1,6-anhydro-2,3,4-tri-*O*-benzoyl-β-D-glucopyranose (**23a**). Hydrogen atoms are omitted for clarity. Ellipsoids are drawn at the 30% probability level. Selected bond lengths (in Å) and angles (in °)[a]: O1–C5 1.425(5)/1.433(1), O1–C1 1.423(4)/1.417(5), O2–C1 1.417(4)/1.417(4), O2–C6 1.436(5)/1.439(4), C5–C6 1.533(5)/1.516(4), C1–C2 1.541(6)/1.507(7), C2–C3 1.513(6)/1.505(6), C3–C4 1.559(6)/1.554(6), C4–C5 1.523(6)/1.507(5), O1–C5–C6 102.2(3)/101.7(2), O2–C6–C5 103.5(3)/104.0(3), C1–O2–C6 107.1(3)/106.1(3), O1–C1–O2 106.1(3)/106.2(3), C1–O1–C5 102.2(3)/101.2(2), C2–C3–C4 113.4(4)/112.7(4), O1–C5–C4 108.7(3)/109.2(2), C5–C4–C3 111.7(3)/111.0(3), C3–C2–C1 112.2(3)/113.2(3), C2–C1–O1 109.3(3)/110.5(3). [a] The values of the two symmetry independent molecules are given separated by a slash.

2.3. Neutral platinum(IV) complexes with monodentately coordinated thioglycoside ligands

Synthesis and NMR spectroscopic characterization. The reaction of *fac*-[$PtMe_3$(OAc-κ^2*O*,*O*′)(Me_2CO)] (**2**) with carbohydrate ligands of type **4** and **5** (Scheme 1) led to the formation of the complexes *fac*-[$PtMe_3$(OAc-κ^2*O*,*O*′)(ch*)] (ch* = ch-SEt **24–28**; ch-STaz **29–35**) (Scheme 4, Table 2). The yellow, white and beige powders, respectively, are moderately air stable and were isolated in yields of 35–89%. The identities of the complexes **24–35** were confirmed by ^{1}H, ^{13}C and ^{195}Pt NMR spectroscopy as well as by IR spectroscopy and high resolution ESI mass spectrometry.

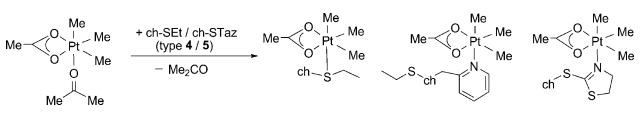

Scheme 4 Syntheses of carbohydrate platinum(IV) complexes *fac*-[$PtMe_3$(OAc-κ^2*O*,*O*′)(ch*)] (ch* = ch-SEt, **24–28**; ch-STaz, **29–35**).

Table 2 Selected NMR and IR spectroscopic data (δ in ppm, J in Hz, ν in cm^{-1}) of the complexes *fac*-[PtMe$_3$(OAc-κ^2*O*,*O*′)(ch*)] (**24–35**)

Complex	ch*	δ_H[a]	δ_C[a]	$^2J_{Pt,H}$[a]	δ_{Pt}	$\nu_{sym.\ (CO_2)}$	$\nu_{asym.\ (CO_2)}$	$\Delta\nu_{CO_2}$
	ch-SEt							
24	**4a**	1.08	−11.2	77.2	−2175	1411	1535	124
25	**4b**	1.07	−11.7	78.0	−2174	1411	1560	149
26	**4c**	1.10	−11.4	77.2	−2173	1409	1550	141
27	**4d**	0.96	−11.3	75.1	−2149	1404	1571	167
28	**4e**	1.15[b]	−10.3	76.4	−2444	1402	1568	166
	ch-STaz							
29	**5a**	1.00	−11.7	77.8	−1910		1534	
30	**5b**	0.91[c]	−11.1	77.2[c]	−1921	1411		
31	**5c**	0.87	−11.3	73.0	−1918	1409	1535	126
32	**5d**	1.17	−11.3	74.4	−1907	1418	1552	134
33	**5e**	1.07	−11.4	75.6	−1904		1533	
34	**5f**	1.08	−11.3	76.4	−1911	1411		
35	**5g**	0.91	−11.5	76.4	−1916		1531	

[a] Chemical shifts and coupling constants refer to the methyl ligands. [b] At −80 °C: 0.98/0.92 ppm. [c] At −50 °C: 0.72/0.78 ppm (74.4/70.4 Hz).

In the ^{1}H NMR spectra, the signals of the PtMe$_3$ protons exhibited broad mean signals at 0.87–1.17 ppm flanked by platinum satellites (singlet plus doublet). The requisite signals in the ^{13}C NMR spectra for **24–35** were found as broad mean singlets. The chemical shifts (δ_H/δ_C) and coupling constants ($^2J_{Pt,H}$) are assembled in Table 2. ^{1}H NMR measurements at −50 °C of the selected samples **28** and **30** showed that the expected split into three separate signals becomes apparent, although a broadening of the signals can be still observed. In the case of trimethylplatinum(IV) complexes with non-functionalized carbohydrate ligands at lower temperatures, three separated sharp signals were observed.[13] As discussed in the previous section, some ^{1}H and ^{13}C NMR signals of the carbohydrate ligands in the complexes **24–35** are also broadened. In contrast to the previously discussed *fac*-[PtMe$_3$(4,4′-R$_2$bpy)(ch-SEt-κ*S*)][BF$_4$] (**8–11**, **13**, **14**) complexes, only marginal CIS's up to 0.12 ppm could be observed for the signals of the CH$_2$ groups of the SEt moieties in the ^{1}H NMR spectra of the complexes **24–27**, having ch-SEt ligands. The chemical shifts for the signals of H1 of the carbohydrate backbones were shifted up to 0.10 ppm. The corresponding CIS's for the carbon atoms of the SEt groups and C1 resonances in the ^{13}C NMR spectra amount up to 1.3 ppm and 1.7 ppm, respectively. For complex **28**, where the ch-SEt ligand **4e** possesses at C6 an additional *N*-donor-site (picoline-2-yl), NOE experiments at −80 °C were performed to examine whether the nitrogen atom is involved in the coordination to platinum. Irradiation into the resonance for H6 of the picoline-2-yl group led to an increase of intensity for one signal of the PtMe$_3$ moiety, stating the spatial surrounding. Thus, a coordination of the nitrogen atom of picoline-2-yl to the platinum atom is likely. In accordance with this, signals of the picoline-2-yl groups were shifted downfield in ^{1}H and ^{13}C NMR spectra up to 0.24 and 2.1 ppm, respectively. Furthermore, the ^{195}Pt chemical shift of complex **28** was found to be about 270 ppm highfield shifted compared to those of complexes **24–27** (−2444 ppm *versus* −2149 to −2175 ppm, Table 2). However, a fast exchange between *N* and *S* coordination in solution could not be definitely ruled out, as indicated by the resonance downfield shift of 0.8 ppm for the CH$_2$ carbon atom signal of the SEt moiety.

The complexes with type **5** ligands *fac*-[PtMe$_3$(OAc-κ^2*O*,*O*′)(ch-STaz)] (**29–35**) showed remarkable upfield shifts for the signals of H1 (0.34–0.50 ppm). The shift differences in ^{1}H NMR spectra of the two methylene proton resonances of the SCH$_2$ (up to 0.21 ppm) and NCH$_2$ (up to 0.30 ppm) were increased in complexes **24–28**. Furthermore, upfield shifts ranging from 2.5–3.2 ppm were observed in the ^{13}C NMR spectra for the signals of the carbon atoms of the SCH$_2$ groups (except **35**). This indicated an *N* coordination of the STaz groups, because the complexes *fac*-[PtMe$_3$(bpy)(ch-STaz-κ*N*)][BF$_4$] (**15–23**), where this coordination mode could be unambiguously proved, showed analogous features. ^{195}Pt NMR chemical shifts of all these complexes between −1910 and −2444 ppm (Table 2) are in the expected range for trimethylplatinum(IV) complexes.[13,16]

High resolution ESI mass spectrometry. High resolution ESI mass spectrometric measurements were performed for complexes **24–35**, which showed in all cases the existence of the molecular cation *fac*-[PtMe$_3$(ch*)]$^+_{-OAc}$ (ch* = ch-SEt, **4a–4e**; ch-STaz; **5a–5g**), exhibiting an isotopic envelope characteristic for monocations containing one platinum atom [natural isotopic composition: ^{190}Pt (0.01%), ^{192}Pt (0.79%), ^{194}Pt (32.9%), ^{195}Pt (33.8%), ^{196}Pt (25.3%) and ^{198}Pt (7.2%)]. The observed isotopic patterns of the molecular cations were in very good agreement with the calculated values. In Fig. 5, the full scan mass spectrum and the expanded spectrum of *fac*-[PtMe$_3$(ch-SEt)]$^+$ (complex [**28** − OAc]$^+$; ch-SEt = **4e**) is shown as an example. Furthermore, other peaks could be detected, which were assigned to be dinuclear complexes *fac*-[(PtMe$_3$)$_2$(OAc)(**4e**)]$^+$ at 1124.3432 *m*/*z*, *fac*-[PtMe$_3$(**4e**)$_2$]$^+$ at 1410.5450 *m*/*z* and *fac*-[(PtMe$_3$)$_2$(OAc)(**4e**)$_2$]$^+$ at 1708.5787 *m*/*z*. According to the NMR spectra, in which the presence of such species can be clearly excluded, these species are formed during the ionization process and/or result from thermal decomposition during the ESI experiment.

IR spectroscopy. IR spectra were recorded to examine the coordination mode of the acetato ligand. The separation ($\Delta\nu_{CO_2}$) between the symmetric and asymmetric stretching band is a suitable tool to distinguish between the different coordination modes.[22] Typical $\Delta\nu_{CO_2}$ values for a monodentate coordination are in general much higher (215–565 cm^{-1} [22]) than those observed in ionic acetates (164–171 cm^{-1} in MOAc, M = alkaline metal[22]). On the other hand, a chelating coordination mode gives rise to $\Delta\nu_{CO_2}$

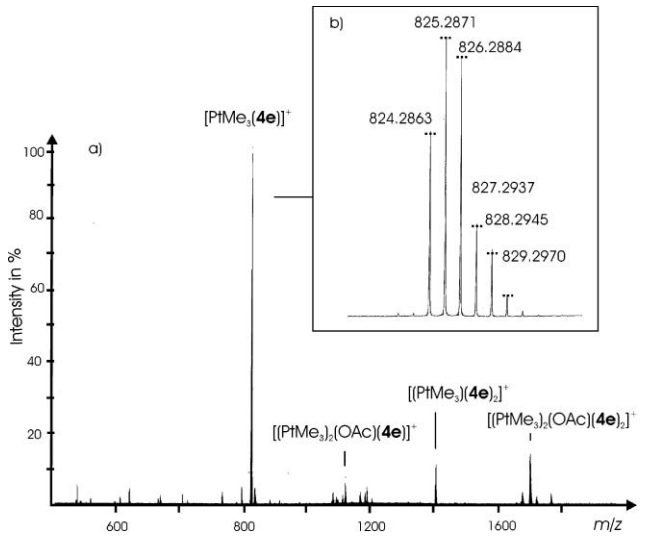

Fig. 5 (a) Positive ESI-mass spectrum of *fac*-[$PtMe_3$(ch-SEt)]$^+$ (complex [**28** – OAc]$^+$; ch-SEt = **4e**). (b) Isotopic pattern of the molecular ion *fac*-[$PtMe_3$(**4e**)]$^+$ at 825.2871 *m*/*z* showing the expected intensity due to the isotopic composition given by horizontal bars.

values, which are similar or significantly lower (65–175 cm^{-1} [22]) in comparison to those for ionic compounds. The stretching frequencies for the asymmetric and symmetric vibrational bands and the differences of those frequencies ($\Delta\nu_{CO_2}$) for the complexes **24–35** are given in Table 2. For the *fac*-[$PtMe_3$(OAc-κ^2*O*,*O*′)(ch-SEt)] complexes **24–28**, $\Delta\nu_{CO_2}$ amounts to 124–167 cm^{-1}, indicating a chelating coordination mode of the acetato ligand. In the case of the *fac*-[$PtMe_3$(OAc-κ^2*O*,*O*′)(ch-STaz)] complexes **29–35**, the assignment of the carboxyl stretching bands is often difficult because of the overlap with the absorption bands of the STaz moiety. Only for complexes **31** and **32** have both the symmetric and asymmetric vibrational bands been assigned unambiguously. The separation by 126 (**31**) and 134 cm^{-1} (**32**), respectively, indicated a chelating coordination mode of the acetato ligand. As shown in Table 2, in the other complexes (**29**, **30**, **33–35**) the position of either ν_{asym} or ν_{sym} is in the same range as that observed in complexes **24–28**, **31** and **32**. Hence, the analogous coordination mode is likely.

2.4. Cationic platinum(IV) complexes with tridentately coordinated thioglycoside ligands

Syntheses and NMR spectroscopic investigations. Complex *fac*-[$PtMe_3(Me_2CO)_3$][BF_4] (**3**) reacted in anhydrous acetone with ligands of type **4** to give mononuclear complexes *fac*-[$PtMe_3$(ch-SEt)][BF_4] (**36–40**) in good yields of 62–87% (Scheme 5, Table 3), where the carbohydrate ligands could coordinate in a tridentate binding fashion. The colorless and beige powders are highly (**36–38**) and moderately (**39**, **40**) air and moisture sensitive, respectively. All complexes were fully characterized by NMR (^{1}H, ^{13}C, ^{195}Pt) spectroscopy, IR spectroscopy and high resolution mass spectroscopy.

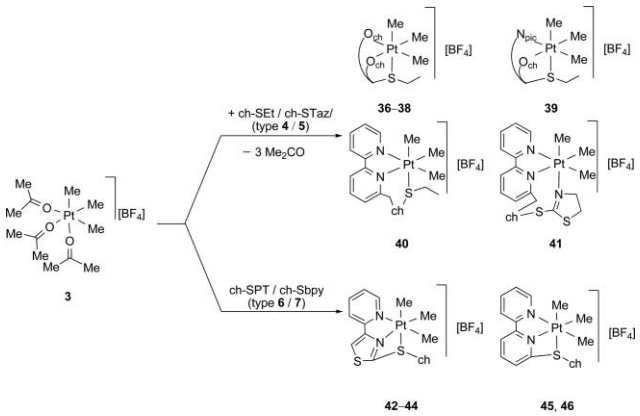

Scheme 5 Syntheses of carbohydrate platinum(IV) complexes *fac*-[$PtMe_3$(ch*)][BF_4] (ch* = ch-SEt, **36–40**; ch-STaz, **41**; ch-SPT, **42–44**; ch-Sbpy, **45**, **46**). N_{pic} = picoline-2-yl.

In the ^{1}H NMR spectra of **36–38** the methyl ligands possessed broad mean signals in a range of 1.18–1.28 ppm flanked by

Table 3 ^{1}H and ^{13}C NMR spectroscopic data (δ in ppm, *J* in Hz) of the methyl ligands and ^{195}Pt chemical shifts of the complexes *fac*-[$PtMe_3$(ch*)][BF_4] (**36–46**)

Complex	ch*	δ_H	δ_C	$^2J_{Pt,H}$	δ_{Pt}
	ch-SEt				
36	**4a**	1.28	−11.2	73.9	−2673
37	**4c**	1.26	−11.7	74.0[a]	−2442
38	**4d**	1.18[a]	−11.3	75.9	−2610
39	**4e**	1.06/1.12	−5.4/−8.6	69.8/72.8	−2068
40	**4f**	0.89/1.26/1.65	4.5/−1.3/−3.8	72.9/69.3/71.1	−2679
	ch-STaz				
41	**5h**	0.81/1.31/1.75	0.2/−4.9/−8.1	73.0/71.4/70.5	−2377
	ch-SPT				
42	**6a**	1.47	−5.8	br	−2154
43	**6b**	1.32	−5.9	br	−2158
44	**6c**	1.41	−5.7	br	−2151
	ch-Sbpy				
45	**7a**	1.45[b]	−3.4	70.5[b]	−2123
46	**7b**	1.33	−3.5	br	−2120

[a] At −50 °C: 0.94/1.07/1.33 ppm (76.9/80.6/79.3 Hz). [b] At −80 °C: 0.94/1.27/1.31 ppm (79.2/65.9/68.4 Hz).

platinum satellites. Chemical shifts and coupling constants are given in Table 3. Measurements at −50 °C using complex **38** as an example, showed the expected split into three separate, sharp signals, revealing the non-equivalence of the methyl ligands. For complexes **39** and **40** having protecting groups at C6 with additional *N*-donor sites (picoline-2-yl, bipyridine-6-yl), the ^{1}H NMR spectra showed two slightly broadened (**39**) and three separate sharp signals (**40**) for the methyl ligands, respectively, flanked by platinum satellites (Table 3). For the signals of the carbohydrate protons in the complexes **36–40**, a broadening of all signals was found for **36–38**. For complexes **39** and **40** only partial broadening was observed. The respective signals for the carbon atoms are partially broadened in all complexes **36–40**. Coordination-induced shifts ($\Delta\delta_H/\Delta\delta_C$) for the methylene group resonances of the SEt moiety (0.16–0.52/0.5–3.2 ppm) and H1 (0.17–0.43/1.3–3.1 ppm) gave evidence that the sulfur atom is coordinated to the platinum atom. The two remaining coordination sites of the platinum atom in **36–38** are, most likely, occupied by any of the following: ring, ether or ester oxygen donor atoms of the carbohydrates. Thus, an $\kappa S,\kappa^2 O,O'$ coordination mode of the carbohydrate ligands in complexes **36–38** can be assumed. In complexes **39** and **40**, the coordination of the picoline-2-yl and bipyridine-6-yl moiety could be clearly seen by a significant downfield shift of the appropriate signals in ^{1}H and ^{13}C NMR spectra up to 0.67 and 5.8 ppm, respectively. This corresponds to an $\kappa S,\kappa N,\kappa O$ (**39**) and $\kappa S,\kappa^2 N,N'$ (**40**) coordination mode of the carbohydrate ligands.

Surprisingly, reactions of *fac*-[$PtMe_3(Me_2CO)_3$][BF_4] (**3**) with ligands of type **5** led to no isolable products. After adding a solution of **3** in acetone to the thioglycoside, in contrast to the common reactions, white precipitates were formed. ^{1}H NMR spectra of the reaction mixtures showed a multitude of products in the carbohydrate area, including the α-hemiacetal. This indicated that a cleavage of the C1–S bonds had occurred in a similar fashion to the decomposition reactions shown in Scheme 3.

To succeed in the formation of *fac*-[$PtMe_3$(ch-STaz)][BF_4] complexes, carbohydrate **5h** having a stabilizing bipyridine-6-yl moiety at C6 (as in **4f**) was selected. In the reaction of *fac*-[$PtMe_3(Me_2CO)_3$][BF_4] (**3**) with **5h** the complex *fac*-[$PtMe_3$(ch-STaz)][BF_4] (**41**; ch-STaz = **5h**) was isolated as a moderately air stable, yellow powder in a yield of 60%. ^{1}H and ^{13}C NMR spectra showed unambiguously the coordination of the bipyridine-6-yl moiety with chemical shift differences of the bipyridine resonances shifted downfield up to 0.92 ppm and 7.1 ppm, respectively. Furthermore, remarkable CIS's of the signals of H1 and C1, which amount to 0.23 (^{1}H NMR) and 4.9 ppm (^{13}C NMR), respectively, are observed. The identity of **41** was also confirmed by high resolution mass spectrometry (Fig. 6). The isotopic pattern of the molecular cation is in a very good agreement with the calculated values.

Obviously, carbohydrates possessing chelating donor groups are the key to yield stable *fac*-[$PtMe_3$(ch*)][BF_4] complexes. Therefore, the carbohydrate classes ch-SPT (type **6**, Scheme 1) and ch-Sbpy (type **7**, Scheme 1), having a chelating group in the aglycone moiety, were included in the subsequent investigations. Reactions of *fac*-[$PtMe_3(Me_2CO)_3$][BF_4] (**3**) with ligands of type **6** and **7** led to the formation of complexes **42–46**, which were isolated as yellow and beige powders, respectively, in yields of 54–75% (Scheme 5). These complexes are stable in anhydrous acetone solutions over a few weeks, without any evidence of decomposition. In chloroform, however, decomposition was observed within 4 days, which might

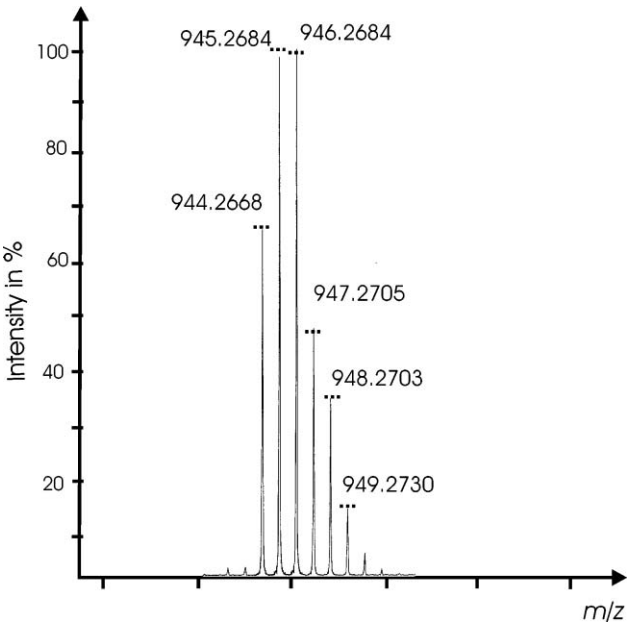

Fig. 6 Isotopic pattern of the cation *fac*-[$PtMe_3$(**5h**)]$^+$ of complex **41** at 945.2684 *m/z*, showing the expected intensity due to the isotopic composition given by horizontal bars.

be caused by the presence of traces of hydrochloric acid. The identities of the complexes were confirmed by ^{1}H, ^{13}C and ^{195}Pt NMR spectroscopy, IR spectroscopy and high resolution ESI mass spectrometry.

The methyl ligands gave broad mean signals in the ^{1}H NMR spectra at 1.32–1.47 ppm, flanked by platinum satellites (Table 3). ^{1}H NMR experiments performed at −80 °C with complex **45** as an example showed the expected split into three separate signals due to the non-equivalence of the methyl ligands. The SPT and Sbpy moieties were unambiguously found to be coordinated to the platinum atom. This was verified by remarkable downfield shifts of the related signals of the protons and carbon atoms up to 1.0 ppm (^{1}H NMR) and 5.1 ppm (^{13}C NMR). The carbohydrate proton resonances are shifted up to 0.41 ppm and are partially broadened, whereas the ^{13}C NMR spectra of compounds **45** and **46** only showed a significant shift of 2.4 (**45**) and 2.9 (**46**) ppm for the signals of C1. Also, a broadening of the resonances of C1 and C2 (**42–46**) and C4 (**44**) can be observed. This indicates that the exocyclic sulfur of the SPT and Sbpy moieties might be the third donor atom coordinated to the platinum atom.

The ESI mass spectra for complexes **42–46** showed the presence of a mononuclear cation *fac*-[$PtMe_3$(ch*)]$^+$ (ch* = ch-SPT, **42–44**; ch-Sbpy, **45**, **46**) containing one platinum atom. The full scan mass spectrum of **43**, depicted in Fig. 7, shows no other platinum-containing cations. The isotopic pattern of the *fac*-[$PtMe_3$(ch-SPT)]$^+$ (ch-SPT = **6b**) cation at 1012.1890 *m/z* is in very good agreement with the calculated values.

3. Conclusion

Platinum(IV) complexes with thioglycoside ligands of the types *fac*-[$PtMe_3$(4,4′-R_2bpy)(ch*)][BF_4] (ch* = ch-SEt, **8–14**; ch-STaz, **15–23**), *fac*-[$PtMe_3$(OAc-$\kappa^2 O,O'$)(ch*)] (ch* = ch-SEt, **24–28**; ch-STaz, **29–35**) and *fac*-[$PtMe_3$(ch*)][BF_4] (ch* = ch-SEt, **36–40**;

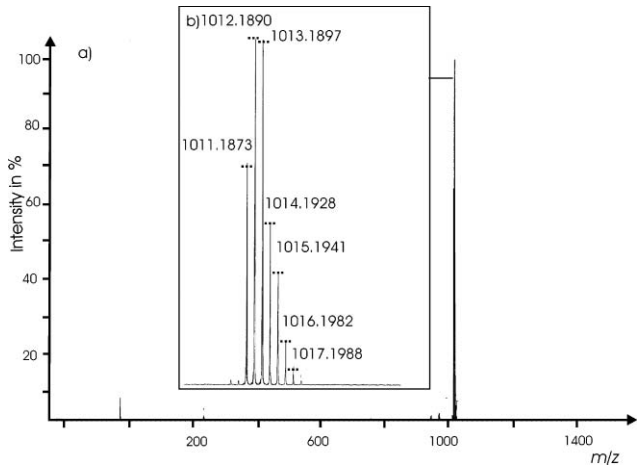

Fig. 7 (a) Positive ESI-mass spectrum of the cation *fac*-[$PtMe_3$(**6b**)]$^+$ of complex **43**. (b) Isotopic pattern of the molecular ion *fac*-[$PtMe_3$(**6b**)]$^+$ at 1012.1890 *m*/*z* showing the expected intensity due to the isotopic composition given by horizontal bars.

ch-STaz, **41**; ch-SPT, **42–44**; ch-Sbpy, **45**, **46**), with the thioglycosides coordinated in a mono- (**8–35**) and tridentate (**36–46**) binding fashion have been synthesized. Despite the kinetic inertness of platinum(IV) complexes due to their low spin d^6 electron configuration, it could be shown that in trimethylplatinum(IV) complexes weakly coordinating ligands like acetone could be smoothly substituted by thioglycosides. These ligand exchange reactions are further supported by the high *trans* effect of the methyl ligands. Furthermore, platinum mediated decomposition of thioglycosides in complexes **21** and **23** involving the cleavage of the C–S glycosidic bonds, yielded the corresponding products **21a** and **23a** (Scheme 3). This result is in accordance with common glycosylation procedures, wherein the glycosidic bond of the glycosyl donor is activated in the first step by adding an electrophilic promoter, such as MeOTf or NIS/TfOH.[2]

As expected from the coordination chemistry perspective, complexes of platinum(IV) in which the thioglycoside ligands have three coordination sites at their disposal (*i.e.* using *fac*-[$PtMe_3(Me_2CO)_3$][BF_4] (**3**) as starting complex) proved to be more air and moisture sensitive than the cationic complexes with bipyridine and the neutral complexes with acetato ligands. Thus, complexes with thioglycoside ligands having only the SEt group as strong donor site could be prepared and characterized (**36–38**), whereas it was not possible with complexes having only the STaz group as the strongest donor site. In the latter cases, a partial cleavage of the glycosidic bonds instead of the anticipated complex formation took place. These cleavage reactions are promoted by the STaz coordination to Pt, as discussed before being a further example for the cleavage of glycosidic bonds by electrophilic promoters.[2] However, it can't be strictly ruled out that these reactions are also influenced by traces of water and/or Ag[BF_4] (present in the reaction mixtures despite using strictly anaerobic conditions and from the *in situ* synthesis of complex **3**, respectively).[23,24] Analogous platinum-mediated reactions, such as cleavage and formation of isopropylidene protecting groups and Schiff bases, were frequently observed in carbohydrate trimethylplatinum(IV) complexes, with non-functionalized carbohydrate ligands.[12,13] In full accord with these findings, we succeeded to get stable complexes of the type *fac*-[$PtMe_3$(ch-STaz)][BF_4] with a derivative having additional strong donor sites in form of a 2,2′-bipyridine-6-yl protecting group at C6 of the carbohydrate moiety (**41**).

For the first time the investigations presented in this study give a deeper insight into the coordination chemistry of thioglycosides to platinum(IV) being a coordination center in a relatively high oxidation number. It has been shown that these ligands can be coordinated not only monodentately through a relatively strong donor site (κ*S* or κ*N*) but also *facial* tridentately using donor sets consisting of one stronger and two weaker donor sites (κ*S*,κ^2*O*,*O*′; *O* = oxygen atom from the carbohydrate backbone), two stronger and one weaker donor sites (κ*S*,κ*N*,κ*O*) or three stronger donor sites (κ*S*,κ^2*N*,*N*′ or κ^3*N*,*N*′,*N*″). Furthermore, coordination of thioglycosides to the highly electrophilic platinum center may give rise to platinum-assisted cleavage of glycosidic C–S bonds, which creates a basis to a deeper understanding of stereocontrolled chemical glycosylations, mediated by metal coordination.[14]

4. Experimental

4.1. General considerations

General considerations. Syntheses were performed, in general, under strictly dehydrated conditions in an argon atmosphere using standard Schlenk techniques. As precipitates, the carbohydrate platinum complexes are stable for a few hours (2–4 h) even in open air, whereas a strictly anhydrous environment was required for handling their solutions in acetone. Acetone and pentane were dried over phosphorus pentoxide followed by 4 Å molecular sieves and $LiAlH_4$, respectively. Diethyl ether was dried over Na-benzophenone. All solvents were distilled prior to use. NMR spectra were obtained with Varian UNITY 500, Gemini 2000 and Bruker 800 spectrometers using solvent signals (^{1}H and ^{13}C NMR spectroscopy) as internal references and $Na_2[PtCl_6]$ ($\delta(^{195}Pt)$ = 0 ppm) as external reference. IR spectra were recorded on a Galaxy Mattson FT IR spectrometer, using KBr pellets. The positive ion high resolution ESI mass spectra were obtained from a Bruker Apex III Fourier transform ion cyclotron resonance (FT-ICR) mass spectrometer (Bruker Daltonics, Billerica, USA) equipped with an Infinity cell, a 7.0 Tesla superconducting magnet (Bruker), a RF-only hexapole ion guide and an external electron spray ion source (Agilent, off axis spray, voltages: endplate, –3.700 V; capillary, –4.200 V; capillary exit, 100 V; skimmer 1, 15.0 V; skimmer 2, 6.0 V). Nitrogen was used as drying gas at 150 °C. The sample solutions were introduced continuously *via* a syringe pump with a flow rate of 120 µl h^{-1}. The data were acquired with 512 *k* data points and zero filled to 2048 *k* by averaging 64 scans. *fac*-[$(PtMe_3I)_4$][14,25] and *fac*-[$PtMe_3I$(bpy)][20] were prepared according to literature methods. All other materials were purchased from commercial sources. Synthesis of *fac*-[$PtMe_3I$(4,4′-^{t}Bu_2bpy)] and its analytical data as well as the NMR and IR spectroscopic data of the carbohydrate platinum complexes **1–46** are available as ESI.† Selected spectroscopic data of complexes **1–46** are given in Table 1–3.

General method for the synthesis of the complexes *fac*-[$PtMe_3$(4,4′-R_2bpy)(ch*)][BF_4](ch* = ch-SEt, R = H: 8–12; R = ^{t}Bu: 13, 14; ch-STaz, R = H: 17–23, R = ^{t}Bu: 15, 16). A suspension of *fac*-[$PtMe_3I$(bpy)] (70.0 mg, 0.14 mmol) or *fac*-[$PtMe_3I$(4,4′-^{t}Bu_2bpy)] (88.9 mg, 0.14 mmol) and Ag[BF_4] (26.5 mg, 0.14 mmol) in acetone (10 ml) was stirred for 30 min

under the absence of light. Precipitated AgI was removed by filtration and the clear, colorless solution of *fac*-[$PtMe_3(Me_2CO)(4,4'$-$R_2bpy)][BF_4]$ (R = H, **1a**; R = ^{t}Bu, **1b**) was added to the respective β-D-thiopyranoside (0.14 mmol). After 5 h the volume of the solution was reduced *in vacuo* to 3 ml and pentane (10 ml) was added. The precipitated solid was filtered, washed with pentane (2 × 2 ml) and dried *in vacuo*.

fac-[$PtMe_3(bpy)(ch\text{-}SEt)][BF_4]$ (***8***, *ch-SEt* = ***4a***). (88 mg, 72%); *m/z* (ESI) 788.2192 ([$PtMe_3$(bpy)(**4a**)]$^+$. $C_{29}H_{41}N_2O_9PtS$ requires 788.2181).

fac-[$PtMe_3(bpy)(ch\text{-}SEt)][BF_4]$ (***9***, *ch-SEt* = ***4b***). (115 mg, 73%); *m/z* (ESI) 788.2193 ([$PtMe_3$(bpy)(**4b**)]$^+$. $C_{29}H_{41}N_2O_9PtS$ requires 788.2181).

fac-[$PtMe_3(bpy)(ch\text{-}SEt)][BF_4]$ (***10***, *ch-SEt* = ***4c***). (102 mg, 65%); *m/z* (ESI) 1036.2805 ([$PtMe_3$(bpy)(**4c**)]$^+$. $C_{49}H_{49}N_2O_9PtS$ requires 1036.2807).

fac-[$PtMe_3(bpy)(ch\text{-}SEt)][BF_4]$ (***11***, *ch-SEt* = ***4d***). (107 mg, 78%); *m/z* (ESI) 980.3623 ([$PtMe_3$(bpy)(**4d**)]$^+$. $C_{49}H_{49}N_2O_9PtS$ requires 980.3636).

fac-[$PtMe_3(bpy)(ch\text{-}SEt)][BF_4]$ (***12***, *ch-SEt* = ***4e***). (90 mg, 68%); *m/z* (ESI) 981.3586 ([$PtMe_3$(bpy)(**4e**)]$^+$. $C_{48}H_{56}N_3O_5PtS$ requires 981.3588).

fac-[$PtMe_3(4,4'$-$^t Bu_2bpy)(ch\text{-}SEt)][BF_4]$ (***13***, *ch-SEt* = ***4a***). (82 mg, 65%); *m/z* (ESI) 900.3437 ([$PtMe_3(4,4'$-$^t Bu_2$bpy)(**4a**)]$^+$. $C_{37}H_{57}N_2O_9PtS$ requires 900.3432).

fac-[$PtMe_3(4,4'$-$^t Bu_2bpy)(ch\text{-}SEt)][BF_4]$ (***14***, *ch-SEt* = **4c**). (72 mg, 54%); *m/z* (ESI) 1148.4030 ([$PtMe_3(4,4'$-$^t Bu_2$bpy)(**6c**)]$^+$. $C_{37}H_{57}N_2O_9PtS$ requires 1148.4058).

fac-[$PtMe_3(4,4'$-$^t Bu_2bpy)(ch\text{-}STaz)][BF_4]$ (***15***, *ch-STaz* = ***5c***). (82 mg, 45%); *m/z* (ESI) 1205.3743 ([$PtMe_3$(**5c**)$(4,4'$-$^t Bu_2$bpy]$^+$. $C_{58}H_{64}N_3O_9PtS_2$ requires 1205.3732).

fac-[$PtMe_3(4,4'$-$^t Bu_2bpy)(ch\text{-}STaz)][BF_4]$ (***16***, *ch-STaz* = ***5g***). (108 mg, 76%); *m/z* (ESI) 1101.3480 ([$PtMe_3(4,4'$-$^t Bu_2$bpy)(**5g**)]$^+$. $C_{58}H_{64}N_3O_9PtS_2$ requires 1101.3470).

fac-[$PtMe_3(bpy)(ch\text{-}STaz)][BF_4]$ (***17***, *ch-STaz* = ***5a***). (130 mg, 85%); *m/z* (ESI) 845.1841 ([$PtMe_3$(bpy)(**5a**)]$^+$. $C_{30}H_{40}N_3O_9PtS_2$ requires 845.1854).

fac-[$PtMe_3(bpy)(ch\text{-}STaz)][BF_4]$ (***18***, *ch-STaz* = ***5b***). (76 mg, 64%); *m/z* (ESI) 1093.2478 ([$PtMe_3$(bpy)(**5b**)]$^+$. $C_{50}H_{48}N_3O_9PtS_2$ requires 1083.2480).

fac-[$PtMe_3(bpy)(ch\text{-}STaz)][BF_4]$ (***19***, *ch-STaz* = ***5c***). (115 mg, 73%); *m/z* (ESI) 1093.2479 ([$PtMe_3$(bpy)(**5c**)]$^+$. $C_{50}H_{48}N_3O_9PtS_2$ requires 1093.2480).

fac-[$PtMe_3(bpy)(ch\text{-}STaz)][BF_4]$ (***20***, *ch-STaz* = ***5d***). (72 mg, 72%); *m/z* (ESI) 1037.3305 ([$PtMe_3$(bpy)(**5d**)]$^+$. $C_{50}H_{48}N_3O_9PtS_2$ requires 1037.3309).

fac-[$PtMe_3(bpy)(ch\text{-}STaz)][BF_4]$ (***21***, *ch-STaz* = ***5e***). (91 mg, 83%); *m/z* (ESI) 733.2074 ([$PtMe_3$(bpy)(**5e**)]$^+$. $C_{26}H_{40}N_3O_5PtS_2$ requires 733.2057).

fac-[$PtMe_3(bpy)(ch\text{-}STaz)][BF_4]$ (***22***, *ch-STaz* = ***5f***). (112 mg, 94%); *m/z* (ESI-MS) 893.2203 ([$PtMe_3$(bpy)(**5f**)]$^+$. $C_{35}H_{44}N_3O_8PtS_2$ requires 893.2218).

fac-[$PtMe_3(bpy)(ch\text{-}STaz)][BF_4]$ (***23***, *ch-STaz* = ***5g***). (91 mg, 83%); *m/z* 989.2243 (ESI) ([$PtMe_3$(bpy)(**5g**)]$^+$. $C_{43}H_{44}N_3O_8PtS_2$ requires 989.2218).

General method for the synthesis of the complexes [$PtMe_3$(OAc-κ$^2O,O'$)(ch*)] (ch* = ch-SEt, 24–28; ch-STaz, 29–35). A suspension of *fac*-[$(PtMe_3I)_4$] (50.0 mg, 0.04 mmol) and AgOAc (23.0 mg, 0.14 mmol) in acetone (10 ml) was stirred for 12 h under the absence of light. Precipitated AgI was removed by filtration and the clear, colorless solution of *fac*-[$PtMe_3$(OAc-κ$^2O,O'$)(Me_2-CO)] (**2**) was directly added to the respective β-D-thiopyranoside (0.14 mmol). After 5 h the volume of the solution was reduced *in vacuo* to 3 ml and pentane (6 ml) was added. The precipitated solid was filtered, washed with pentane (2 × 2 ml) and dried *in vacuo*.

fac-[$PtMe_3(OAc$-κ$^2O,O')(ch\text{-}SEt)$] (***24***, *ch-SEt* = ***4a***). (55 mg, 57%); *m/z* (ESI) 632.1498 ([$PtMe_3$(OAc-κ$^2O,O'$)(**4a**)]$^+_{-OAc}$. $C_{30}H_{40}N_3O_9PtS_2$ requires 632.1493).

fac-[$PtMe_3(OAc$-κ$^2O,O')(ch\text{-}SEt)$] (***25***, *ch-SEt* = ***4b***). (62 mg, 70%); *m/z* (ESI) 632.1498 [$PtMe_3$(OAc-κ$^2O,O'$)(**4b**)]$^+_{-OAc}$. $C_{30}H_{40}N_3O_9PtS_2$ requires 632.1493).

fac-[$PtMe_3(OAc$-κ$^2O,O')(ch\text{-}SEt)$] (***26***, *ch-SEt* = ***4c***). (64 mg, 54%); *m/z* (ESI) 880.2108 ([$PtMe_3$(OAc-κO,O')(**4c**)]$^+_{-OAc}$. $C_{30}H_{40}N_3O_9PtS_2$ requires 880.2119).

fac-[$PtMe_3(OAc$-κ$^2O,O')(ch\text{-}SEt)$] (***27***, *ch-SEt* = **4d**). (64 mg, 54%); *m/z* 824.2939 ([$PtMe_3$(OAc-κ$^2O,O'$)(**4d**)]$^+_{-OAc}$. $C_{39}H_{49}O_5PtS$ requires 824.2948).

fac-[$PtMe_3(OAc$-κ$^2O,O')(ch\text{-}SEt)$] (***28***, *ch-SEt* = ***4e***). (75 mg, 58%); *m/z* (ESI) 825.2871 ([$PtMe_3$(OAc-κ$^2O,O'$)(**4e**)]$^+_{-OAc}$. $C_{38}H_{48}NO_5PtS$ requires 825.2901).

fac-[$PtMe_3(OAc$-κ$^2O,O')(ch\text{-}STaz)$] (***29***, *ch-STaz* = ***5a***). (93 mg, 89%); *m/z* (ESI) 689.1172 ([$PtMe_3$(OAc-κ$^2O,O'$)(**5a**)]$^+_{-OAc}$. $C_{20}H_{32}NO_9PtS_2$ requires 689.1166).

fac-[$PtMe_3(OAc$-κ$^2O,O')(ch\text{-}STaz)$] (***30***, *ch-STaz* = ***5b***). (120 mg, 86%); *m/z* (ESI) 937.1753 ([$PtMe_3$(OAc-κ$^2O,O'$)(**5b**)]$^+_{-OAc}$. $C_{40}H_{40}NO_9PtS_2$ requires 937.1792).

fac-[$PtMe_3(OAc$-κ$^2O,O')(ch\text{-}STaz)$] (***31***, *ch-STaz* = ***5c***). (86 mg, 68%); *m/z* (ESI) 937.1789 ([$PtMe_3$(OAc-κ$^2O,O'$)(**4e**)]$^+_{-OAc}$. $C_{16}H_{32}NO_5PtS_2$ requires 937.1792).

fac-[$PtMe_3(OAc$-κ$^2O,O')(ch\text{-}STaz)$] (***32***, *ch-STaz* = ***5d***). (102 mg, 80%); *m/z* (ESI) 881.2630 ([$PtMe_3$(OAc-κ$^2O,O'$)(**5d**)]$^+_{-OAc}$. $C_{40}H_{48}NO_5PtS_2$ requires 881.2622).

fac-[$PtMe_3(OAc$-κ$^2O,O')(ch\text{-}STaz)$] (***33***, *ch-STaz* = ***5e***). (30 mg, 35%); *m/z* (ESI) 577.1368 [$PtMe_3$(OAc-κ$^2O,O'$)(**5e**)]$^+_{-OAc}$. $C_{16}H_{32}NO_5PtS_2$ requires 577.1370).

fac-[$PtMe_3(OAc$-κ$^2O,O')(ch\text{-}STaz)$] (***34***, *ch-STaz* = ***5f***). (67 mg, 60%); *m/z* (ESI) 737.1525 ([$PtMe_3$(OAc-κ$^2O,O'$)(**5f**)]$^+_{-OAc}$. $C_{25}H_{36}NO_8PtS_2$ requires 737.1530).

fac-[$PtMe_3(OAc$-κ$^2O,O')(ch\text{-}STaz)$] (***35***, *ch-STaz* = ***5g***). (44 mg, 35%); *m/z* (ESI) 833.1553 ([$PtMe_3$(OAc-κ$^2O,O'$)(**5g**)]$^+_{-OAc}$. $C_{33}H_{36}NO_8PtS_2$ requires 833.1530).

General method for the synthesis of the complexes [$PtMe_3$(ch*)]-[BF_4] (ch* = ch-SEt, 36–40; ch-STaz, 41, ch-SPT, 42–44, ch-Sbpy, 45, 46). A suspension of *fac*-[$(PtMe_3I)_4$] (70.0 mg, 0.04 mmol) and Ag[BF_4] (26.5 mg, 0.14 mmol) in acetone (10 ml) was stirred for 30 min under the absence of light. Precipitated AgI was removed by filtration and the clear, colorless solution of *fac*-[$PtMe_3(Me_2CO)_3][BF_4]$ (**3**) was directly added to the respective β-D-thiopyranoside (0.14 mmol). After 5 h the volume of the solution was reduced *in vacuo* to 3 ml and pentane (10 ml) was added. The precipitated solid was filtered, washed with pentane (2 × 2 ml) and dried *in vacuo*.

fac-[$PtMe_3(ch\text{-}SEt)][BF_4]$ (***36***, *ch-SEt* = ***4a***). (42 mg, 87%); *m/z* (ESI) 632.1492 [$PtMe_3$(**4a**)]$^+$. $C_{19}H_{33}O_9PtS$ requires 632.1493).

fac-[$PtMe_3(ch\text{-}SEt)][BF_4]$ (***37***, *ch-SEt* = ***4c***). (40 mg, 62%); *m/z* (ESI) 880.2115 ([$PtMe_3$(**4c**)]$^+$. $C_{39}H_{41}O_9PtS$ requires 880.2119).

Table 4 Crystal data, data collection and refinement parameters of *fac*-[$PtMe_3$(bpy)(ch-STaz-κ*N*)][BF_4] (**19**, ch-STaz = **5c**), *fac*-[$PtMe_3$(bpy)(STazH-κ*S*)][BF_4] (**21a**) and 1,6-anhydro-2,3,4-tri-*O*-benzoyl-β-D-glucopyranose (**23a**)

	19	**21a**	**23a**
Formula	$C_{50}H_{48}BF_4N_3O_9PtS_2$	$C_{16}H_{22}BF_4N_3PtS_2$	$C_{27}H_{22}O_8$
FW	1180.94	602.39	474.45
Crystal system	Tetragonal	Monoclinic	Triclinic
Space group	$P4_12_12$	$P2_1/c$	$P1$
a/Å	22.1611(9)	13.2216(5)	9.6936(8)
b/Å	22.1611(9)	12.6149(5)	11.011(1)
c/Å	43.735(2)	12.8474(5)	11.449(1)
α/°			66.414(4)
β/°		115.776(2)	89.999(4)
γ/°			89.894(4)
V/Å^3	21479(2)	1929.6(1)	1119.9(2)
Z	16	4	2
$D_{calc.}$/g cm^{-3}	1.461	2.074	1.407
T/K	100(2)	100(2)	100(2)
μ/mm^{-1}	6.194	7.532	0.104
θ/°	4.47–61.49	1.71–36.00	1.94–26.44
F(000)	9472	1160	496
Index ranges	$-23 \le h \le 20$ $-25 \le k \le 25$ $-49 \le l \le 47$	$-21 \le h \le 21$ $-19 \le k \le 20$ $-21 \le l \le 21$	$-11 \le h \le 12$ $-13 \le k \le 13$ $-14 \le l \le 14$
Reflns collected	66857	56461	28835
Reflns obs [$I > 2\sigma(I)$]	4582	7098	6186
Reflns independent	16385 ($R_{int} = 0.1328$)	9070 ($R_{int} = 0.0643$)	8089 ($R_{int} = 0.0699$)
Data/restraints/parameters	16385/1332/1103	9070/1/257	8089/3/604
GOF(F^2)	0.617	1.034	1.003
R_1, wR_2 ($I > 2\sigma$)	0.0481/0.0785	0.0347/0.0757	0.0602/0.1447
R_1, wR_2 (all data)	0.1755/0.0966	0.0529/0.0828	0.0810/0.1593
Largest diff. peak and hole/e Å^{-3}	1.009 and –0.519	1.958 and –1.058	0.358 and –0.350
Flack parameter	–0.044(9)		0.4(10)

fac-[*PtMe*$_3$(*ch-SEt*)][BF_4] (***38***, *ch-SEt* = ***4d***). (53 mg, 70%); *m*/*z* (ESI) 824.2948 ([$PtMe_3$(**4d**)]$^+$. $C_{39}H_{49}O_5PtS$ requires 824.2948).

fac-[*PtMe*$_3$(*ch-SEt*)][BF_4] (***39***, *ch-SEt* = ***4e***). (92 mg, 72%); *m*/*z* (ESI) 825.2903 ([$PtMe_3$(**4e**)]$^+$. $C_{38}H_{48}NO_5PtS$ requires 825.2901).

fac-[*PtMe*$_3$(*ch-SEt*)][BF_4] (***40***, *ch-SEt* = ***4f***). (118 mg, 85%); *m*/*z* (ESI) 888.2940 ([$PtMe_3$(**4f**)]$^+$. $C_{43}H_{48}N_3O_5PtS_2$ requires 888.3010).

fac-[*PtMe*$_3$(*ch-STaz*)][BF_4] (***41***, *ch-STaz* = ***5h***). (87 mg, 60%); *m*/*z* (ESI) 945.2684 ([$PtMe_3$(**5h**)]$^+$. $C_{43}H_{48}N_3O_5PtS_2$ requires 945.2683).

fac-[*PtMe*$_3$(*ch-SPT*)][BF_4] (***42***, *ch-SPT* = ***6a***). (77 mg, 65%); *m*/*z* (ESI) 764.1262 ([$PtMe_3$(**6a**)]$^+$. $C_{25}H_{33}N_2O_9PtS_2$ requires 764.1275).

fac-[*PtMe*$_3$(*ch-SPT*)][BF_4] (***43***, *ch-SPT* = ***6b***). (83 mg, 54%); *m*/*z* (ESI) 1012.1890 ([$PtMe_3$(**6b**)]$^+$. $C_{45}H_{41}N_2O_9PtS_2$ requires 1012.1901).

fac-[*PtMe*$_3$(*ch-SPT*)][BF_4] (***44***, *ch-SPT* = ***6c***). (98 mg, 67%); *m*/*z* (ESI) 956.2702 ([$PtMe_3$(**6c**)]$^+$. $C_{45}H_{49}N_2O_5PtS_2$ requires 956.2731).

fac-[*PtMe*$_3$(*ch-Sbpy*)][BF_4] (***45***, *ch-Sbpy* = ***7a***). (89 mg, 75%); *m*/*z* (ESI) 758.1679 ([$PtMe_3$(**7a**)]$^+$. $C_{27}H_{35}N_2O_9PtS$ requires 758.1711).

fac-[*PtMe*$_3$(*ch-Sbpy*)][BF_4] (***46***, *ch-Sbpy* = ***7b***). (101 mg, 66%); *m*/*z* (ESI) 1006.2331 ([$PtMe_3$(**7b**)]$^+$. $C_{47}H_{43}N_2O_9PtS$ requires 1006.2337).

4.2. X-Ray crystallography†

Single crystals of *fac*-[$PtMe_3$(bpy)(ch-STaz-κ*N*)][BF_4] (ch-STaz = **5c**, **19**), *fac*-[$PtMe_3$(bpy)(STazH-κ*S*)][BF_4] (**21a**) and 1,6-anhydro-2,3,4-tri-*O*-benzoyl-glucopyranose (**23a**) for X-ray diffraction measurements were obtained from acetone/ether/THF (1 : 1 : 1) (**19**) and acetone/ether/pentane solutions (1 : 1 : 1) (**21a**, **23a**), respectively. Intensity data were collected on a Oxford Gemini S diffractometer with Cu-Kα radiation (λ = 1.54184 Å, graphite monochromator) at 100(2) K (**19**) and on a Bruker Apex II Kappa diffractometer with Mo-Kα radiation (λ = 0.71073 Å, graphite monochromator) at 100(2) K (**21a**, **23a**). A summary of the crystallographic data, the data collection parameters and the refinement parameters is given in Table 4. Numerical (**21a**) and multiscan (**23a**) absorption corrections were applied (T_{min}/T_{max} 0.18/0.55, **21a**; T_{min}/T_{max} 0.97/0.98, **23a**). The structures were solved by direct methods with SHELXS-97[26] and refined using full matrix least square routines against F^2 with SHELXL-97.[26] Non-hydrogen atoms were refined with anisotropic displacement parameters. The hydrogen atom attached to nitrogen in **21a** was found in the difference Fourier map and refined freely. All other hydrogen atoms were positioned geometrically and refined with isotropic displacement parameters according to the "riding model". Although measured at 100 K with Cu-Kα radiation the small sized needle-like crystals (0.3 × 0.03 × 0.03 mm) of complex **19** showed only a weak reflectivity resulting in a limited quality of the structure solution. The required fixing of disordered groups (phenyl rings and $[BF_4]^-$ anions) for the refinement of **19**, led to the comparatively high number of restraints. The fluoroatom F4 of the tetrafluoroborate anion in complex **21a** was found to be disordered over two equally occupied positions.

4.3. Computational details

DFT calculations of compounds were carried out by the Gaussian 03 program package[27] using the hybrid functional B3LYP.[28] The

6-311G(d,p) basis sets as implemented in Gaussian 03 were employed for main group atoms. The valence shell of platinum has been approximated by a split valence basis set too; for its core orbitals an effective core potential in combination with consideration of relativistic effects has been used.[29] The appropriateness of the functional in combination with the basis sets and effective core potential used for reliable interpretation of structural and energetic aspects of related platinum complexes has been demonstrated.[30] All systems were fully optimized without any symmetry restrictions. The resulting geometries were characterized as equilibrium structures by the analysis of the force constants of normal vibrations. Solvent effects were considered according to the polarized continuum model as implemented in Gaussian 03.[31]

Acknowledgements

Financial support from the National Science Foundation (award CHE-0547566 to AVD), the National Institute of General Medical Sciences (award GM077170 to AVD), and gifts of chemicals by Merck (Darmstadt) is gratefully acknowledged. Special thanks to Prof. J. Balbach and Dipl.-Phys. M. Kovermann (Martin-Luther-Universität Halle-Wittenberg) for the NMR spectroscopic measurements on the 800 MHz spectrometer.

References

1 R. A. Dwek, *Chem. Rev.*, 1996, **96**, 683.
2 T. Lindhorst, *Essentials of Carbohydrate Chemistry*, Wiley-VCH, Weinheim, 2nd edn, 2003, 175 pp.
3 T. Storr, M. Merkel, G. X. Song-Zhao, L. E. Scott, D. E. Green, M. L. Bowen, K. H. Thompson, B. O. Patrick, H. J. Schugar and C. Orvig, *J. Am. Chem. Soc.*, 2007, **129**, 7453.
4 (*a*) D. J. Hoffman and R. L. Whistler, *Biochemistry*, 1968, **7**, 4479; (*b*) R. L. Whistler and W. C. Lake, *Biochem. J.*, 1972, **130**, 919; (*c*) B. Hellman, Å. Lernmark, J. Sehlin, I.-B. Täljedal and R. L. Whistler, *Biochem. Pharmacol.*, 1973, **22**, 29; (*d*) J. R. Zysk, A. A. Bushway, R. L. Whistler and W. W. Carlton, *J. Reprod. Fertil.*, 1975, **45**, 69.
5 (*a*) J. H. Kim, S. H. Kim, E. W. Hahn and C. W. Song, *Science*, 1978, **200**, 206.
6 (*a*) H. Hashimoto, T. Fujimori and H. Yuasa, *J. Carbohydr. Chem.*, 1990, **9**, 683; (*b*) C.-H. Wong, Y. Ichikawa, T. Krach, C. Gautheron-Le Narvor, D. P. Dumas and G. C. Look, *J. Am. Chem. Soc.*, 1991, **113**, 8137; (*c*) B. D. Johnston and B. M. Pinto, *J. Org. Chem.*, 1998, **63**, 5797.
7 (*a*) M. Takeuchi, M. Yoshikawa, R. Sasaki and H. Chiba, *Agric. Biol. Chem.*, 1982, **46**, 2741; (*b*) G. Guo, G. Li, D. Liu, Q.-J. Yang, Y. Liu, Y.-K. Jing and L.-X. Zhao, *Molecules*, 2008, **13**, 1487; (*c*) M. Singer, M. Lopez, L. F. Bornaghi, A. Innocenti, D. Vullo, C. T. Supuran and S.-A. Poulsen, *Bioorg. Med. Chem. Lett.*, 2009, **19**, 2273; (*d*) N. M. Khalifa, M. M. Ramla, A. E.-G. E. Amr and M. M. Abdulla, *Phosphorus, Sulfur Silicon Relat. Elem.*, 2008, **183**, 3046.
8 S. Yano, *Coord. Chem. Rev.*, 1988, **92**, 113.
9 D. M. Whitfield, S. Stojkovski and B. Sarkar, *Coord. Chem. Rev.*, 1993, **122**, 171.
10 (*a*) J. Petrig, R. Schibli, C. Dumas, R. Alberto and P. A. Schubiger, *Chem.–Eur. J.*, 2001, **7**, 1868; (*b*) D. J. Yang, C.-G. Kim, N. R. Schechter, A. Azhdarinia, D.-F. Yu, C.-S. Oh, J. L. Bryant, J.-J. Won, E. E. Kim and D. A. Podoloff, *Radiology*, 2003, **226**, 465; (*c*) T. Storr, Y. Sugai, C. A. Barta, Y. Mikata, M. J. Adam, S. Yano and C. Orvig, *Inorg. Chem.*, 2005, **44**, 2698; (*d*) T. Storr, C. L. Fisher, Y. Mikata, S. Yano, M. J. Adam and C. Orvig, *Dalton Trans.*, 2005, 654.
11 Y. Mikata, Y. Shinohara, K. Yoneda, Y. Nakamura, I. Brudziñska, T. Tanase, T. Kitayama, R. Takagi, T. Okamoto, I. Kinoshita, M. Doe, C. Orvig and S. Yano, *Bioorg. Med. Chem. Lett.*, 2001, **11**, 3045.
12 D. Steinborn and H. Junicke, *Chem. Rev.*, 2000, **100**, 4283.
13 (*a*) H. Junicke, C. Bruhn, D. Ströhl, R. Kluge and D. Steinborn, *Inorg. Chem.*, 1998, **37**, 4603; (*b*) D. Steinborn, H. Junicke and C. Bruhn, *Angew. Chem., Int. Ed. Engl.*, 1997, **36**, 2686; (*c*) H. Junicke, C. Bruhn, R. Kluge, A. S. Serianni and D. Steinborn, *J. Am. Chem. Soc.*, 1999, **121**, 6232; (*d*) H. Junicke, R. Kluge and D. Steinborn, *J. Inorg. Biochem.*, 2000, **81**, 43.
14 P. Pornsuriyasak, C. Vetter, S. Kaeothip, M. Kovermann, J. Balbach, D. Steinborn and A. V. Demchenko, *Chem. Commun.*, 2009, 6379.
15 Cambridge Structural Database (CSD) Version 5.30 2008, University Chemical Laboratory, Cambridge (England).
16 (*a*) T. G. Appleton, H. C. Clark and L. E. Manzer, *Coord. Chem. Rev.*, 1973, **10**, 335; (*b*) C. Vetter, C. Wagner, J. Schmidt and D. Steinborn, *Inorg. Chim. Acta*, 2006, **359**, 4326.
17 R. Bucourt, *Top. Stereochem.*, 1974, **8**, 159.
18 (*a*) C. Vetter, C. Wagner, G. N. Kaluđerović, R. Paschke and D. Steinborn, *Inorg. Chim. Acta*, 2009, **362**, 189; (*b*) C. Vetter, G. N. Kaluđerović, R. Paschke and D. Steinborn, *Inorg. Chim. Acta*, 2010, DOI: 10.1016/j.ica.2010.03.079.
19 (*a*) C. Vetter, diploma thesis, Martin-Luther-Universität Halle-Wittenberg, Halle 2005; (*b*) R. Lindner, G. N. Kaluđerović, R. Paschke, C. Wagner and D. Steinborn, *Polyhedron*, 2008, **27**, 914.
20 (*a*) E. S. Raper, R. E. Oughtred and I. W. Nowell, *Inorg. Chim. Acta*, 1983, **77**, L89; (*b*) H. T. Flakus, A. Miros and P. G. Jones, *Spectrochim. Acta, Part A*, 2002, **58**, 225; (*c*) R. S. Corrêa, S. A. Santana, R. Salloum, R. M. Silva and A. C. Doriguetto, *Acta Crystallogr., Sect. C: Cryst. Struct. Commun.*, 2006, **62**, o115.
21 C. Janiak, *J. Chem. Soc., Dalton Trans.*, 2000, 3885.
22 (*a*) G. B. Deacon and R. J. Phillips, *Coord. Chem. Rev.*, 1980, **33**, 227; (*b*) L. C. Francesconi, D. R. Corbin, A. W. Clauss, D. N. Hendrickson and G. D. Stucky, *Inorg. Chem.*, 1981, **20**, 2059; (*c*) M. Gasgnier and A. Petit, *J. Mater. Sci.*, 1994, **29**, 6479.
23 S. Kaeothip, P. Pornsuriyasak and A. V. Demchenko, *Tetrahedron Lett.*, 2008, **49**, 1542.
24 A. V. Demchenko, P. Pornsuriyasak, C. De Meo and N. N. Malysheva, *Angew. Chem., Int. Ed.*, 2004, **43**, 3069.
25 J. C. Baldwin and W. C. Kaska, *Inorg. Chem.*, 1975, **14**, 2020.
26 G. M. Sheldrick, *Acta Crystallogr., Sect. A: Found. Crystallogr.*, 2008, **64**, 112.
27 M. J. Frisch, G. W. Trucks, H. B. Schlegel, G. E. Scuseria, M. A. Robb, J. R. Cheeseman, J. A. Montgomery, Jr., T. Vreven, K. N. Kudin, J. C. Burant, J. M. Millam, S. S. Iyengar, J. Tomasi, V. Barone, B. Mennucci, M. Cossi, G. Scalmani, N. Rega, G. A. Petersson, H. Nakatsuji, M. Hada, M. Ehara, K. Toyota, R. Fukuda, J. Hasegawa, M. Ishida, T. Nakajima, Y. Honda, O. Kitao, H. Nakai, M. Klene, X. Li, J. E. Knox, H. P. Hratchian, J. B. Cross, V. Bakken, C. Adamo, J. Jaramillo, R. Gomperts, R. E. Stratmann, O. Yazyev, A. J. Austin, R. Cammi, C. Pomelli, J. Ochterski, P. Y. Ayala, K. Morokuma, G. A. Voth, P. Salvador, J. J. Dannenberg, V. G. Zakrzewski, S. Dapprich, A. D. Daniels, M. C. Strain, O. Farkas, D. K. Malick, A. D. Rabuck, K. Raghavachari, J. B. Foresman, J. V. Ortiz, Q. Cui, A. G. Baboul, S. Clifford, J. Cioslowski, B. B. Stefanov, G. Liu, A. Liashenko, P. Piskorz, I. Komaromi, R. L. Martin, D. J. Fox, T. Keith, M. A. Al-Laham, C. Y. Peng, A. Nanayakkara, M. Challacombe, P. M. W. Gill, B. G. Johnson, W. Chen, M. W. Wong, C. Gonzalez and J. A. Pople, *GAUSSIAN 03 (Revision B.04)*, Gaussian, Inc., Wallingford, CT, 2004.
28 (*a*) A. D. Becke, *Phys. Rev. A: At., Mol., Opt. Phys.*, 1988, **38**, 3098; (*b*) A. D. Becke, *J. Chem. Phys.*, 1993, **98**, 5648; (*c*) C. Lee, W. Yang and R. G. Parr, *Phys. Rev. B: Condens. Matt. Mater. Phys.*, 1988, **37**, 785; (*d*) P. J. Stephens, F. J. Devlin, C. F. Chabalowski and M. J. Frisch, *J. Phys. Chem.*, 1994, **98**, 11623.
29 (*a*) D. Andrae, U. Häußermann, M. Dolg, H. Stoll and H. Preuss, *Theor. Chim. Acta*, 1990, **77**, 123; (*b*) See http://bse.pnl.gov/bse/portal.
30 (*a*) K. Nordhoff and D. Steinborn, *Organometallics*, 2001, **20**, 1408; (*b*) T. Gosavi, C. Wagner, H. Schmidt and D. Steinborn, *J. Organomet. Chem.*, 2005, **690**, 3229; (*c*) M. Werner, T. Lis, C. Bruhn, R. Lindner and D. Steinborn, *Organometallics*, 2006, **25**, 5946; (*d*) D. Steinborn and S. Schwieger, *Chem.–Eur. J.*, 2007, **13**, 9668; (*e*) S. Schwieger, R. Herzog, C. Wagner and D. Steinborn, *J. Organomet. Chem.*, 2009, **694**, 3548; (*f*) R. Lindner, C. Wagner and D. Steinborn, *J. Am. Chem. Soc.*, 2009, **131**, 8861.
31 (*a*) E. Cancés, B. Mennucci and J. Tomasi, *J. Chem. Phys.*, 1997, **107**, 3032; (*b*) M. Cossi, V. Barone, B. Mennucci and J. Tomasi, *Chem. Phys. Lett.*, 1998, **286**, 253; (*c*) B. Mennucci and J. Tomasi, *J. Chem. Phys.*, 1997, **106**, 5151.

